

31. S. S. Golden, M. S. Nalty, D.-C. Cho, *J. Bacteriol.* **171**, 4707 (1989).
 32. A. M. R. Wilimotte and W. T. Stam, *J. Gen. Microbiol.* **130**, 2737 (1984).
 33. Y. Ouyang, thesis, Vanderbilt University (1998).
 34. T. Kondo *et al.*, *Science* **266**, 1233 (1994).
 35. R. Smith, B. Wiese, M. Wojzynski, D. Davison, K. Worley, *Genome Res.* **6**, 454 (1996).
 36. S.-H. Wu and J. C. Lagarias, unpublished data.
 37. We thank C. Strayer, M. Straume, and V. Cassone for assistance with statistical analysis, C. Johnson and Y. Ouyang for the *purf::luc* reporter construct, D. Hodgson for the gentamycin resistance cassette, C. Inoue and K. Okamoto for information that influenced the design of phase-resetting experiments, and C. Lagarias for help in aligning phytochrome chromophore binding domains. This work was supported in part by grants from the NIH

(GM37040) and NSF (MCB9513367) to S.S.G. and the Human Frontier Science Program grant to S.S.G. and T.K. (with co-principal investigators C. Johnson and M. Ishiura). M.K. and S.B.W. were supported by postdoctoral fellowships from the Japan Society for the Promotion of Science and NIH National Research Service Award, respectively.

21 April 2000; accepted 20 June 2000

Cloning of the *Arabidopsis* Clock Gene *TOC1*, an Autoregulatory Response Regulator Homolog

Carl Strayer,^{1,2} Tokitaka Oyama,¹ Thomas F. Schultz,¹ Ramanujam Raman,¹ David E. Somers,^{1*} Paloma Más,¹ Satchidananda Panda,¹ Joel A. Kreps,^{1†} Steve A. Kay^{1‡}

The *toc1* mutation causes shortened circadian rhythms in light-grown *Arabidopsis* plants. Here, we report the same *toc1* effect in the absence of light input to the clock. We also show that *TOC1* controls photoperiodic flowering response through clock function. The *TOC1* gene was isolated and found to encode a nuclear protein containing an atypical response regulator receiver domain and two motifs that suggest a role in transcriptional regulation: a basic motif conserved within the *CONSTANS* family of transcription factors and an acidic domain. *TOC1* is itself circadianly regulated and participates in a feedback loop to control its own expression.

The endogenous circadian clock enables organisms to anticipate and adapt to daily variations in the environment and to temporally coordinate internal processes. In animals, fungi, and bacteria, genetic screens for altered circadian rhythms have revealed molecular clock components. The generally conserved core mechanism consists of autoregulatory transcriptional loops in which positive factors act on genes encoding negative factors that in turn feed back to block their own expression (1). Although plant models have proven valuable for understanding circadian input and output pathways, our understanding of processes at the core of the plant circadian system is lacking.

We therefore executed a screen for rhythm mutants in *Arabidopsis*, from which we identified the *toc1* (*timing of CAB expression*) mutant (2). The defining phenotype is a shortened period of luciferase-reported *CAB* gene expression (~21 hours, versus ~24.5

hours in the wild type) under constant light conditions (LL). All clock phenotypes tested are similarly affected by the *toc1-1* mutation, which is semidominant, as are mutant alleles of diverse clock genes (1–3). Moreover, the effects of the *toc1-1* mutation are specific to the clock system, with no defects seen, for instance, in clock-independent light responses (3). This is noteworthy because disruption of photoreceptors and phototransduction components that participate in clock entrainment can alter period in LL (4, 5). However, perturbations of these components produce specific, differential effects depending on the quality and quantity of light, whereas the *toc1-1* effect is essentially the same in all light conditions (3). To further address this issue, we assayed the bioluminescence rhythm of *toc1-1* and wild-type seedlings during extended dark incubation (DD) using a new reporter, *ccr2::luc*. *CCR2* (*COLD-CIRCADIAN RHYTHM-RNA-BINDING 2*) is a clock-controlled gene whose LL expression rhythm is shortened by the *toc1-1* mutation (6). The *ccr2::luc* reporter (including a luciferase gene fusion) reveals that *toc1-1* has a similar effect on the period of gene expression in DD (Fig. 1), consistent with a role for *TOC1* outside of light input pathway(s) to the clock.

Mutation of *TOC1* also affects photoperiodic regulation of floral induction. Wild-type

Arabidopsis flowers earlier in long days [16 hours light, 8 hours dark (16:8 LD)] than in short days (8:16 LD), but this differential response is greatly reduced in *toc1-1* (3). This phenotype is likely the result of clock-based misinterpretation of photoperiodic information in *toc1-1* rather than direct effects of *toc1-1* on floral induction pathways. To test this possibility, we measured the transition to flowering of *toc1-1* lines grown in LD cycles of 21 hours total duration, where the environmental period (*T*) more closely matched the period of the endogenous clock (τ) (Fig. 2). Correct photoperiodic response was restored in *toc1-1* plants grown in this regime, where *toc1-1* plants flowered much later in short days (7:14 LD) than in long days (14:7 LD). The *toc1-1* flowering defect therefore can be fully explained by its circadian defect. The cause is not simply incorrect measurement of light or dark intervals: Mutant plants given 7 hours light in a 24-hour period (7:17 LD) also flowered early (Fig. 2). These data, combined with results of experiments measuring gene expression in *toc1-1* and wild-type plants entrained to altered *T* cycles (3), also suggest a possible mechanism underlying this defect: incorrect modulation of phase and/or waveform of clock-controlled regulatory factors when τ varies greatly from *T*.

To further investigate its role in the *Arabidopsis* circadian system, we isolated the *TOC1* gene. Genetic mapping delimited

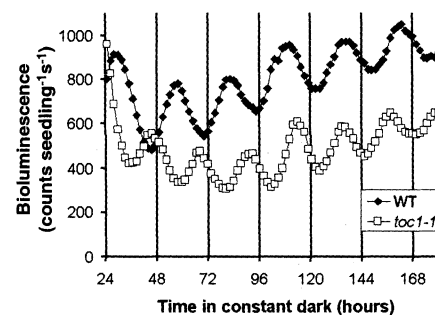


Fig. 1. Bioluminescence rhythms from *toc1-1* and wild-type seedlings in constant darkness (DD). *ccr2::luc* transgenic seedlings (7) were grown in 12:12 LD for 8 days before transfer to DD. Bioluminescence was recorded at the indicated times (7). Traces represent averages of 21 to 23 seedlings from each line. Period estimates (variance-weighted means \pm variance-weighted SD) for each line were calculated as described (26, 27): wild type = 27.5 ± 1.16 hours, *toc1-1* = 22.3 ± 0.39 hours.

¹Department of Cell Biology, Scripps Research Institute, La Jolla, CA 92037, USA. ²Department of Biology, University of Virginia, Charlottesville, VA 22903, USA.

*Present address: Department of Plant Biology, Ohio State University, Columbus, OH 43210, USA.

†Present address: Novartis Agricultural Discovery Institute, San Diego, CA 92121, USA.

‡To whom correspondence should be addressed. E-mail: stevek@scripps.edu

TOC1 to a 78-kb interval on chromosome 5 (7). Sequencing of *toc1-1* and wild-type DNA from this region identified a missense mutation in the *toc1-1* allele of one candidate gene (Fig. 3). We confirmed this gene as *TOC1* by identifying a nucleotide change in a second mutant allele, *toc1-2* (Fig. 3). The *cab2::luc* rhythm defect of *toc1-2* homozy-

gotes is similar to that of *toc1-1* homozygotes (LL period \approx 22 hours) (8); however, the *toc1-2* allele appears to be recessive (1). The *toc1-2* mutation changes the last nucleotide in exon 1, and one result is preferential splicing at a site 13 nucleotides 3' to the normal donor site with a concomitant reduction in correctly spliced transcript (Fig. 3, A and E) (7). Quantitative reverse-transcription polymerase chain reaction (RT-PCR) revealed that correctly spliced transcripts are 6% of the total in *toc1-2*, versus 96% of the total in the wild type (Fig. 3E). The incorrectly spliced transcript would encode a truncated protein of only 59 residues. Taken together, these results suggest that *toc1-2* is a hypomorph, the loss-of-function phenotype is short period, and the semidominant *toc1-1* allele is therefore likely an antimorph.

The predicted *TOC1* protein contains several notable features. At the NH₂-terminus, *TOC1* contains a motif similar to the receiver domain of response regulators from two-component signal transduction systems (Fig. 3, B and C). Typically in these systems, the first component, a sensor kinase, perceives changes in environmental conditions and propagates signals by autophosphorylation of a conserved histidine residue (9). This phos-

phate is subsequently transferred to an aspartate within the receiver domain of a response regulator, which then effects the response, often a change in the transcriptional state of target genes (9). However, *TOC1* would be unique among characterized response regulators in that two of three invariant residues required for normal response are substituted. In CheY, an *Escherichia coli* response regulator, Asp⁵⁷ (D₁ in Fig. 3C), is the normal site of phosphorylation by its cognate sensor kinase (CheA), and Asp¹³ and Lys¹⁰⁹ (D₂ and K in Fig. 3C) are also crucial for normal phosphorelay and function (9). Residues corresponding to D₁ and D₂ are changed to Glu and Asn, respectively, in *TOC1*. About 14 response regulator homologs have been identified in *Arabidopsis*, which can be classified as type A or type B on the basis of primary structure (Fig. 3C) (10). *TOC1* defines a new class because of the atypical primary structure of its receiver-like domain. We have identified several *TOC1-LIKE* (TL) sequences in the *Arabidopsis* genome (Fig. 3, C and D) (11) that are defined by this atypical motif and another feature, a distinctive COOH-terminal motif first identified within the *CONSTANS* family of plant transcription factors. The *CONSTANS* (*CO*) locus controls photo-

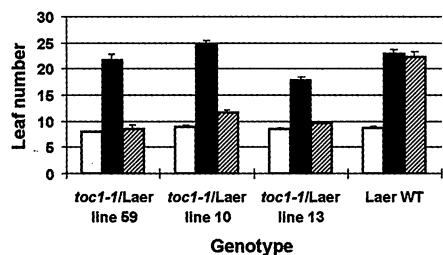


Fig. 2. Photoperiodic response of *toc1-1* plants in LD cycles of different period. Wild-type seedlings [ecotype Landsberg (Laer)] or seedlings homozygous for the *toc1-1* (C24) allele introgressed into Laer (*toc1-1/Laer*) were grown in various photocycles as described (3, 28) ($n = 12$ to 22 for each condition). Initiation of flowering was defined as rosette leaf number at flower bolt height of 1 cm. Open bars, long days (14:7); solid bars, short days (7:14); striped bars, short days (7:17). Error bars denote SEM.

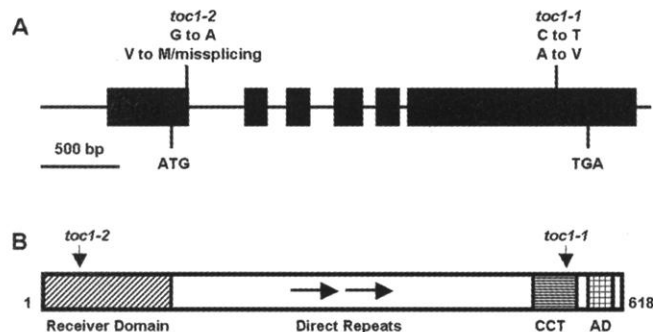


Fig. 3. Structure of *TOC1* gene and gene products. **(A)** Gene organization of *TOC1*. Black boxes represent exons. Positions of start and stop codons and mutations in *TOC1* are indicated. **(B)** Predicted protein structure of *TOC1*. **(C)** Comparison of receiver domains of *TOC1* (GenBank accession no. AF272039), TL1 (AF272040), representative *Arabidopsis* response regulator homologs ARR2 (AB016472) (type B) and ARR4 (AF057282) (type A), and CheY (M13463) (9, 10, 29). Residues identical to *TOC1* are in black boxes; similar residues are in gray boxes. An asterisk indicates the residue mutated in *toc1-1*; # and + indicate residues mutated in *co5* and *co7*, respectively (15). **(D)** Comparison of CCT motifs of *TOC1*, TL1, *Arabidopsis* CO (CAA64407), *Arabidopsis* COL1 (Y10555), *Arabidopsis* COL2 (L81119), and *Brassica* CO9a (Bn CO: AF016011). Sequences are highlighted as in (C). An asterisk indicates the residue mutated in *toc1-1*; # and + indicate residues mutated in *co5* and *co7*, respectively (15). **(E)** RT-PCR analysis of *TOC1* transcripts. Autoradiograph from polyacrylamide gel electrophoresis (PAGE) analysis of products from quantitative RT-PCR (7) is shown at the left. A cartoon represents RT-PCR products from the two splice products. The lower band derives from the correctly spliced product containing the complete open reading frame. Nucleotide sequences surrounding the splice junctions (slashes) from each species from the *toc1-2* allele are shown at the right. Nucleotides included in the species represented in the upper band are underlined. The mutated nucleotide and amino acid residues changed in *toc1-2* are boxed in gray. Single-letter abbreviations for amino acid residues: A, Ala; C, Cys; D, Asp; E, Glu; F, Phe; G, Gly; H, His; I, Ile; K, Lys; L, Leu; M, Met; N, Asn; P, Pro; Q, Gln; R, Arg; S, Ser; T, Thr; V, Val; W, Trp; and Y, Tyr.

C

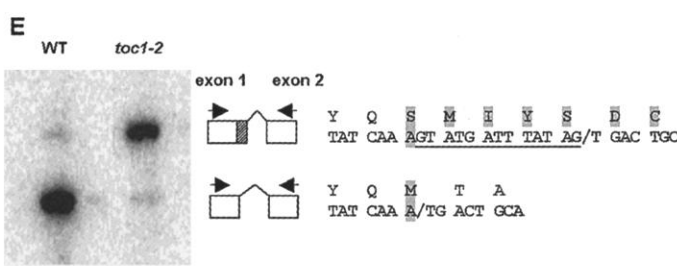
Protein	Residue	Sequence
<i>TOC1</i>	19	VRIILCNDSTSLGGEVFTLLSECSY-DVTAVKRSARQVIDALNIEGPD---
TL1	37	IRVLLVESQYSTRQIITALLRRCQY-RVAVSDGLAAAEVVEKESHN---
ARR2	28	LRVIVVDDPPFCMILERMIMTCLY-RVTKCNRAESALSLRKNKN---
ARR4	34	NHVAVVDSLVDRIVIERLRITSC-KVTAVDSGWRALFPLDNEKASA---
CheY	6	LKFLVVDVDFSTMRRIURNLRLELGFNNVEEAEDGVDALNRIQAG-----

Protein	Residue	Sequence
<i>TOC1</i>	65	-----IDIIILAEHDLPMAGKMKRYITRDKDLRRIPVIMMSRQDEVVY
TL1	83	-----IDIIILAEHDLPMAGKMKRYITRDKDLRRIPVIMMSRQDEVVY
ARR2	73	-----GFDLVI SDVHDDMDGCELEHV---GLEMDIPVIMMSADSKSV
ARR4	83	EFDRLLKVDLIIIDYCPGEMTCYELKKKESSNFREPVPVIMSENVLTR
CheY	50	-----GYGFVLSQWNNMDELELKTTRADGMSALEPLVIVTAEARKEN

Protein	Residue	Sequence
<i>TOC1</i>	109	VVKCKLIGADYLVKPHRTNELNLNLWVWRRRRLMG
TL1	127	VVKCKLIGADYLVKPHRTNELNLNLWVWRRRRLMG
ARR2	115	VVKCVTHGAVDYLKPHVRIEALRNKHVYVKKRNEW
ARR4	133	VDRCLEEGADLLKPKVKLADVKRRRSHLTKDVKLSN
CheY	95	ITAAQAQASGTVVVRPFATATBEELNKIKFEKLG

D

Protein	Residue	Sequence
<i>TOC1</i>	531	DREBAILKFRKRNRQCFDKKIRYVNRRLAERRPRVKGQFVRKVN
TL1	415	SREBAILKFRKRNRQCFDKKIRYVNRRLAERRPRVKGQFVRKVN
CONSTANS	304	MDREARVLYRREKRRTRRFRTIRYASRRAYAEIRPRVNGREAKREI
COL1	284	RDREARVLYRREKRRTRRFRTIRYASRRAYAEIRPRVNGREAKREI
COL2	276	MDREARVLYRREKRRTRRFRTIRYASRRAYAEIRPRVNGREAKREI
Bn CO	293	MDREARVLYRREKRRTRRFRTIRYASRRAYAEIRPRVNGREAKREI
Consensus		RE R K R F K R Y R K AE RPR G F



REPORTS

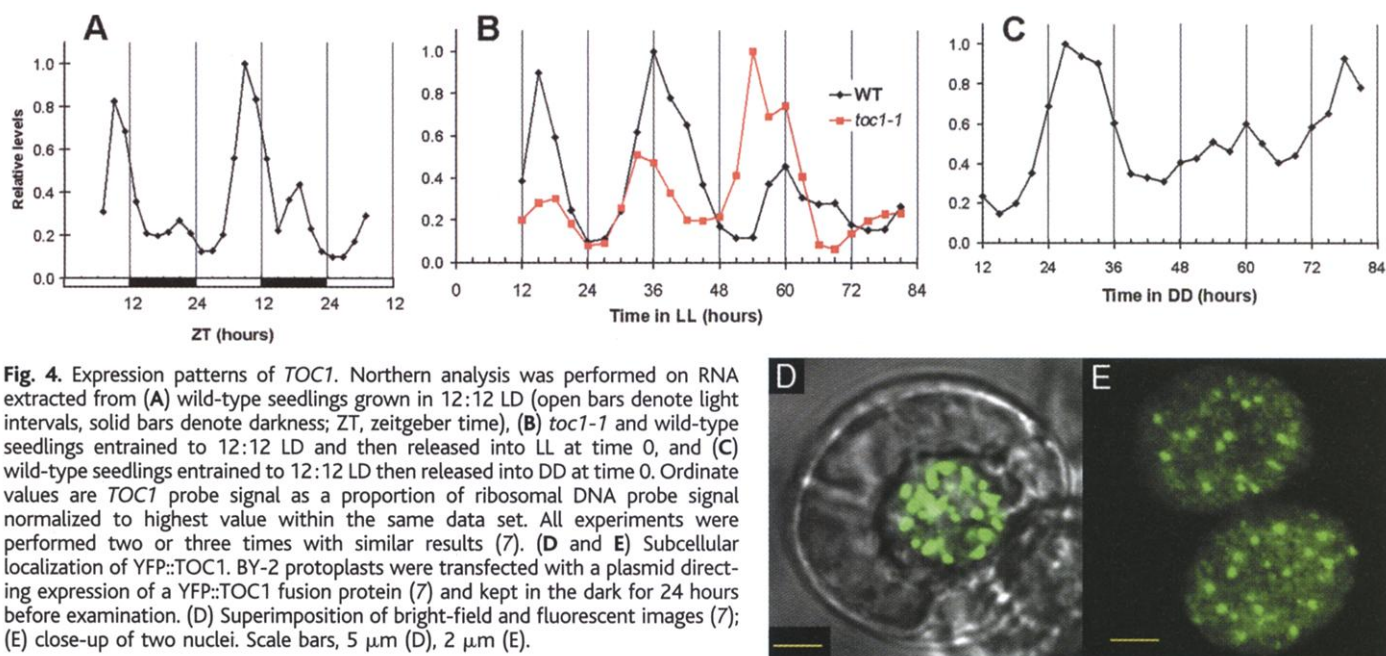


Fig. 4. Expression patterns of *TOC1*. Northern analysis was performed on RNA extracted from (A) wild-type seedlings grown in 12:12 LD (open bars denote light intervals, solid bars denote darkness; ZT, zeitgeber time), (B) *toc1-1* and wild-type seedlings entrained to 12:12 LD and then released into LL at time 0, and (C) wild-type seedlings entrained to 12:12 LD then released into DD at time 0. Ordinate values are *TOC1* probe signal as a proportion of ribosomal DNA probe signal normalized to highest value within the same data set. All experiments were performed two or three times with similar results (7). (D and E) Subcellular localization of YFP::TOC1. BY-2 protoplasts were transfected with a plasmid directing expression of a YFP::TOC1 fusion protein (7) and kept in the dark for 24 hours before examination. (D) Superimposition of bright-field and fluorescent images (7); (E) close-up of two nuclei. Scale bars, 5 μ m (D), 2 μ m (E).

periodic flowering response (12). Structurally, the CONSTANS-LIKE (COL) family is typified by the presence of this highly conserved COOH-terminal domain, herein termed the CCT (CO, COL, and TOC1) motif, and two NH₂-terminal zinc finger domains (12–14). The CCT motif is ~45 amino acids, rich in basic residues, and contains a putative nuclear localization signal in the NH₂-terminal half (14). *toc1-1* is mutated at a residue within the second half of the CCT motif, and proximal residues are mutated in two *co* alleles (Fig. 3D) (15). Immediately downstream of the CCT motif is a region rich in acidic residues, a feature common to a number of transcriptional activators (16). The last identifiable feature within TOC1 is an almost perfect direct repeat of 47 amino acids in the center of the protein, of unknown function.

Messenger RNA levels of *TOC1* cycled robustly in light-dark cycles, peaking in the late day (Fig. 4A). Changes in *TOC1* levels did not coincide with dawn or dusk transitions, nor were *TOC1* transcript levels acutely light-induced (17). In the absence of entraining signals, robust cycling persisted throughout an LL time course (Fig. 4B). Notably, the period of the *TOC1* circadian rhythm was shortened in the *toc1-1* mutant, demonstrating that *TOC1* products feed back to affect their own expression (Fig. 4B). The *TOC1* rhythm was bimodal in LD conditions, and aspects of this were evident in the LL time course (Fig. 4, A and B). One explanation is that *TOC1* expression is always biphasic. Another possibility is that the phase of *TOC1* expression is distinct in two different populations of cells or tissues, as has been shown for circadian

genes in other organisms (18). In DD, the rhythm of mRNA expression dampened after one cycle, although mean levels were maintained (Fig. 4C).

As predicted from the pervasive effect of *TOC1* mutation, a *toc1::luc* transcriptional reporter was expressed in all organs of seedlings and mature plants (17, 19). We used translational fusions to yellow fluorescent protein (YFP) to investigate the subcellular localization of TOC1. In transiently transfected tobacco cells incubated in the dark, YFP::TOC1 appeared exclusively in the nucleus in a distinctive speckled pattern (Fig. 4, D and E). This pattern suggests TOC1 participation in functionally important complexes such as transcriptosomes, spliceosomes, or proteosomes (20). The same pattern was observed in transfected cells kept in the light (17), arguing against light-dependent differential partitioning of TOC1, such as we have shown for the circadian photoreceptor dCRY, which forms similar patterns in insect nuclei (21).

Although it is premature to unequivocally place *TOC1* in a central pacemaker, the identification of TOC1 molecular targets and partners will elucidate its specific role. Interestingly, PAS (PER, ARNT, SIM) domains found in several clock proteins show sequence similarity to two-component sensor domains (4, 22). Other clock-associated proteins are similar to sensor kinases and exhibit kinase activity (23, 24). More typical sensor kinase homologs have also been identified in *Arabidopsis* (25). However, considering the atypical nature of its receiver domain, TOC1 may not be involved in an orthodox phosphorelay.

Note added in proof: Several *Arabidopsis*

sequences were recently recognized as encoding atypical response regulator homologs, including one corresponding to *TOC1* (30).

References and Notes

1. J. C. Dunlap, *Cell* **96**, 271 (1999).
2. A. J. Millar, I. A. Carré, C. A. Strayer, N.-H. Chua, S. A. Kay, *Science* **267**, 1161 (1995).
3. D. E. Somers, A. A. R. Webb, M. Pearson, S. Kay, *Development* **125**, 485 (1998).
4. D. E. Somers, T. F. Schultz, M. Milnamow, S. A. Kay, *Cell* **101**, 319 (2000).
5. D. E. Somers, P. F. Devlin, S. A. Kay, *Science* **282**, 1488 (1998).
6. J. A. Kreps and A. E. Simon, *Plant Cell* **9**, 297 (1997).
7. For additional data, see Science Online (www.sciencemag.org/feature/data/1051477.shl).
8. Period phenotype was determined as described (2) for F₃ plants from the first backcross to the parental line (C24).
9. J. B. Stock, A. M. Stock, J. M. Mottonen, *Nature* **344**, 395 (1991).
10. A. Imamura *et al.*, *Plant Cell Physiol.* **40**, 733 (1999).
11. AC005310, AB019231, AB025641.5, and AL162973 (GenBank accession numbers) were identified by BLAST searches of *Arabidopsis* genomic sequence. A cDNA corresponding to AC005310 (*TL1*) was amplified by RT-PCR (7).
12. J. Putterill, F. Robson, K. Lee, R. Simon, G. Coupland, *Cell* **80**, 847 (1995).
13. L. S. Robert, F. Robson, A. Sharpe, D. Lydiate, G. Coupland, *Plant Mol. Biol.* **37**, 763 (1998).
14. J. Putterill *et al.*, *Plant Physiol.* **114**, 396 (1997).
15. F. Robson and G. Coupland, personal communication.
16. W. D. Cress and S. J. Treizeberg, *Science* **251**, 87 (1991).
17. C. Strayer, T. Oyama, P. Más, S. A. Kay, unpublished data.
18. M. Kaneko, C. Helfrich-Förster, J. C. Hall, *J. Neurosci.* **17**, 6745 (1997).
19. Transgenic *Arabidopsis* plants carrying *toc1::luc*⁺ (2.3 kb of *TOC1* upstream sequence fused to the luciferase gene) were imaged (7). Bioluminescent organs included roots, stems, leaves, flowers, and siliques.
20. A. G. Matera, *Trends Cell Biol.* **9**, 302 (1999).
21. M. F. Ceriani *et al.*, *Science* **285**, 553 (1999).
22. J. L. Pellequer, K. A. Wager-Smith, S. A. Kay, E. D. Getzoff, *Proc. Natl. Acad. Sci. U.S.A.* **95**, 5884 (1998).
23. H. Iwasaki *et al.*, *Cell* **101**, 223 (2000).
24. K. C. Yeh and J. C. Lagarias, *Proc. Natl. Acad. Sci. U.S.A.* **95**, 13976 (1998).

25. T. Urao, K. Yamaguchi-Shinozaki, K. Shinozaki, *Trends Plant Sci.* **5**, 67 (2000).
 26. J. D. Plautz et al., *J. Biol. Rhythms* **12**, 204 (1997).
 27. A. J. Millar, M. Straume, J. Chory, N.-H. Chua, S. A. Kay, *Science* **267**, 1163 (1995).
 28. Short-day fluence rates were $180 \mu\text{mol m}^{-2} \text{s}^{-1}$; long-day fluence rates were $90 \mu\text{mol m}^{-2} \text{s}^{-1}$.
 29. A cDNA with similarity to CO that corresponds to *TOC1* was reported recently [S. Kurup, H. D. Jones, M. J. Holdsworth, *Plant J.* **21**, 143 (2000)].
 30. S. Makino et al., *Plant Cell Physiol.* **41**, 791 (2000).
 31. Thanks to T. Kuhlmann and A. Schopke for technical assistance; J. Takahashi, T. Stevens, and M. Milnamow for sequencing; J. Bender and T. Caspar for marker

information; and Kay lab members for support. Supported by NIH grant GM 56006 and the NSF Center for Biological Timing (S.A.K.), fellowships from BP America and NSF-Graduate Research Training Program (C.S.), Human Frontier Science Program (T.O.), and NSF grants DBI-9804249 (T.F.S.) and BIR-9403981 (D.E.S.).

19 April 2000; accepted 13 June 2000

Pif1p Helicase, a Catalytic Inhibitor of Telomerase in Yeast

J.-Q. Zhou, E. K. Monson,* S. -C. Teng,* V. P. Schulz,*† V. A. Zakian‡

Mutations in the yeast *Saccharomyces cerevisiae* *PIF1* gene, which encodes a 5'-to-3' DNA helicase, cause telomere lengthening and a large increase in the formation rate of new telomeres. Here, we show that Pif1p acts by inhibiting telomerase rather than telomere-telomere recombination, and this inhibition requires the helicase activity of Pif1p. Overexpression of enzymatically active Pif1p causes telomere shortening. Thus, Pif1p is a catalytic inhibitor of telomerase-mediated telomere lengthening. Because Pif1p is associated with telomeric DNA in vivo, its effects on telomeres are likely direct. Pif1p-like helicases are found in diverse organisms, including humans. We propose that Pif1p-mediated inhibition of telomerase promotes genetic stability by suppressing telomerase-mediated healing of double-strand breaks.

PIF1 is a nonessential *Saccharomyces* gene that encodes a 5'-to-3' DNA helicase (1). Mutations in *PIF1* affect telomeres in three ways: telomeres from *pif1* mutant cells are longer than wild-type telomeres; healing of double-strand breaks by telomere addition occurs much more often in *pif1* cells than in wild-type cells; and *pif1* cells but not wild-type cells add telomeric DNA to sites that have very little resemblance to telomeric DNA (2). These data suggest that Pif1p is an inhibitor of telomere lengthening. Pif1p also affects mitochondrial (1) and ribosomal DNA (3).

There are two mechanisms that can lengthen the ~300-base pair (bp) tracts of yeast telomeric $C_{1-3}A/TG_{1-3}$ DNA: telomerase (4) and telomere-telomere recombination (5). In the absence of genes required for telomerase such as *TLC1*, which encodes telomerase RNA (6), and *EST1*, which encodes a telomerase RNA binding protein (7), telomeric DNA gets shorter and shorter, the cultures senesce, and most cells eventually die. Lengthening of telomeres by recombination requires the continued presence of Rad52p (5). If Pif1p inhibits telomere-telomere recombination, telomere lengthening will not occur in a *pif1 rad52* strain, and a *pif1 tlc1* (or *est1*) strain might not senesce or would senesce more slowly due to activation of the recombina-

tional pathway for telomere maintenance. If Pif1p inhibits telomerase, telomere lengthening would not occur in *pif1 tlc1* or *pif1 est1* strains. To distinguish between these possibilities, we constructed singly and doubly mutant strains of the appropriate genotypes and examined telomere lengths (8). Because telomeres were at least as long in a *pif1 rad52* as in a *pif1* strain (Fig. 1A), the effects of Pif1p did not require Rad52p. In contrast,

telomere lengthening did not occur in either a *pif1 tlc1* (Fig. 1B) or a *pif1 est1* strain (9). In addition, lack of Pif1p did not bypass or even delay the senescence phenotype of cells lacking telomerase (Fig. 1C). Thus, Pif1p inhibits a telomerase-dependent pathway of telomere lengthening.

To determine if the helicase function of Pif1p is required to inhibit telomere lengthening, we used site-directed mutagenesis to modify the invariant lysine in the ATP-binding domain to either alanine (K264A) or arginine (K264R) (10), as this residue is essential for the activity of other helicases (11). Both the wild-type and the K264A mutant version of Pif1p were expressed in Sf9 insect cells infected with recombinant baculovirus, purified to near homogeneity (Fig. 2A), and their activities assayed in vitro. Whereas wild-type Pif1p catalyzed unwinding of a 17-base, [³²P]end-radiolabeled oligonucleotide annealed to a M13 single-strand circle, the K264A allele had no helicase activity in this assay (Fig. 2B).

To determine the phenotype of cells that lacked Pif1p helicase activity, strains with only the K264A or K264R allele were constructed (12). DNA was prepared from cells carrying these mutant alleles, as well as from

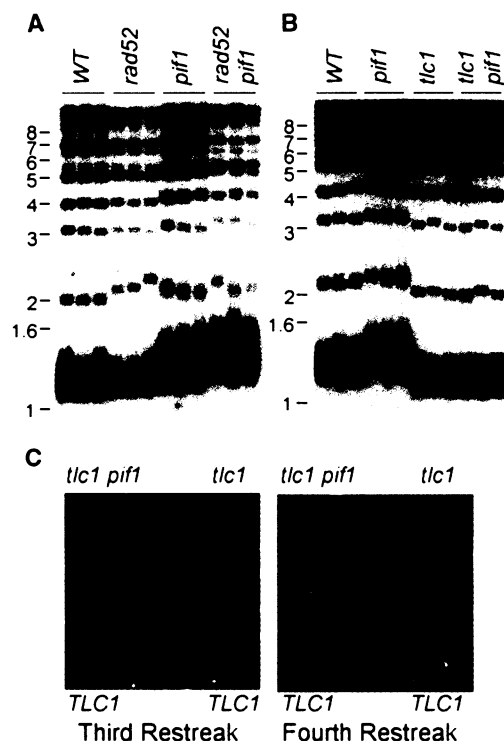


Fig. 1. Pif1p inhibits telomerase, not telomere-telomere recombination. (A) DNA was prepared from three independent transformants from otherwise isogenic strains of the indicated genotypes. The DNA was digested with Xho I and analyzed by Southern hybridization using a $C_{1-3}A/TG_{1-3}$ telomeric probe here and in (B). The *pif1-m2* allele, which affects telomeric but not mitochondrial DNA (2), was used here and in (B) and (C). (B) A diploid strain heterozygous at both *TLC1* and *PIF1* was sporulated, tetrads were dissected, and the genotype of the spore products was determined. DNA was isolated from independent spores with the indicated genotypes ~30 cell divisions after sporulation. (C) Individual spores from tetrads obtained as in (B) were streaked on rich medium and grown to single colonies (~25 cell divisions). Individual colonies were restreaked repeatedly. The third and fourth restreaks after sporulation are shown for the four spore products from one of nine tetrads examined.

Department of Molecular Biology, Princeton University, Princeton, NJ 08544-1014, USA.

*These authors contributed equally to this work.

†Present address: Genaissance Pharmaceuticals, Five Science Park, New Haven, CT 06511, USA.

‡To whom correspondence should be addressed: E-mail: vzakian@molbio.princeton.edu